Safety of a Child, in a Vehicle Side Crash, with Three Restraint Systems

Abbas Talimian, Jan Vychytil, Luděk Hynčík, Tomasz Bońkowski

Biomechanical human body models, New Technologies Research Centre, University of West Bohemia, Univerzitní 2732/8, 301 00 Plzeň, Czech Republic, talimian@ntc.zcu.cz, jvychyti@ntc.zcu.cz, hyncik@ntc.zcu.cz, tomasz@ntc.zcu.cz

Abstract: Child safety is the main concern for parents, while driving a vehicle, with a child on board. Appropriate child restraint systems (CRSs) optimistically lessen injuries and reduce the mortality rate of children in accidents. This study compares child safety in a near-side crash with three different restraint systems: safety vest, and three- and four-point seatbelts. A six-year-old child is modelled by scaling a reference human model. The child is in an upright posture and located on a simplified child seat. The child seat itself is affixed to a deformable car seat that is made from fully deformable foam. The foam is validated to be used in crash analysis. The interior of the child seat is also covered by a layer of this foam. Seatbelts and the safety vest are made from standard seatbelt membrane material. Simulations were done for the near-side crash by a sled test regarding the side barrier crash pulse in the virtual performance solution (VPS). Outcomes indicate that a four-point seatbelt and safety vest, can provide relatively safer conditions for a child, in a near-side crash, than a three-point seatbelt, from a thorax injury point of view. This is the direct consequence of distributing the load over the thorax. Using a four-point seatbelt puts delay in the thorax injury and helps to use other safety means to reduce injuries on the body. The assumed geometry of the safety vest is not appropriate and causes the model's pelvis injury grade to be worse than that seen with three-point seatbelts.

Keywords: child model; Virthuman; child restraint systems; sled test; injury assessment

1   Introduction

Child occupant injury prevention in motor vehicles is one of the most important public health issues around the globe. Regardless of the continuous increase in the number of vehicles on the road, a downward trend is seen in children's death rate as a result of improvements in child restraint systems [4]. However, up to half of the traffic casualties in high-income countries, are children. For instance, in 2004 almost 40% of fatal road traffic deaths recorded in the Czech Republic were

related to children [20]. Consequently, designing suitable child restraint systems (CRSs) is a must in the developing car industry. Besides an applicable design, the correct usage of CRSs raises the chance of reducing fatal injury risk. Child safety seats could reduce the fatal injury risk of infants and toddlers in passenger vehicles by 71% and 54% respectively [29]. It is also important to select an applicable restraint system according to the child occupant's age and weight because it can effectively reduce the deaths of young children, even up to 70% [20].

Three restraint systems are widely used for children, in vehicles [25]. Rear-facing restraint is suggested for infants. It is quite common to have toddlers in forward-facing restraints. For older children, it is recommended to use a booster that is located on the vehicle seat [1]. The usage of a booster helps to fit the vehicle's seatbelt on the child's thorax. Of course, it is possible to use a combination of CRS types for some children as they grow up. Unfortunately, some vehicle users are not familiar with installing and using standard seatbelts with a child restraint system such as that for a toddler who is on a booster [22]. Incorrect usage of a seatbelt with a restraint system potentially increases the risk of injury for a child who is aged 11 years and below in a vehicle crash [19]. On the other hand, when CRSs are used correctly, it lowers children's death risk by 28%, in comparison with an occasion in which a child just fastens a vehicle seatbelt [5].

Children's body parts are in a state of growth and they are more vulnerable to injuries in vehicle crash scenarios, compared to adults [20]. Regarding the national highway traffic safety administration (NHTSA), children have to use boosters until they reach age 8 unless they are taller than 1.45 m [24]. According to [19], vehicle users are advised to put their children in front-facing CRS with booster seats to be able to use the seatbelts which are designed for adult passengers [2]. A seatbelt is an ideal one if it can securely distribute pressure over either a wider area of the child's chest or hard bones rather than soft internal organs during a crash [24, 28]. The pressure distribution over the child's chest efficiently decreases its body part injury in a crash. When a vehicle brakes, the interaction between a seatbelt and a child's posture will be problematic [3]. Therefore, two belt-positioning booster seats were tested to meet federal motor vehicle safety standards: the high-back and the backless or low-back booster seats. A belt-positioning booster seat is useful, as it positions a child in a vehicle seat in such a way that a standard belt will fit across the child's thorax and lap.

From this context, a safety vest conceptual design, is introduced based on current research [13]. The safety vest ends are connected to the child seat and have a zipper in front. It is easy for a driver to use. The driver can put a child on the seat and close the vest's front, with a zipper. In addition, the safety vest distributes pressure over a child's thorax while a child fastens a seatbelt –the shoulder strap applies extra pressure on some thorax segments which are under it. In the present study, a child model is located on a simplified child seat model. Subsequently, the

body's injury levels for the safety vest are compared with three-point and four-point seatbelts in a side crash.

The present study models a child's body, by scaling the reference model Virthuman [16]. This model is a useful and reliable model for having a fast calculation process and predicting the injury risk on different body parts in different crash scenarios [15]. It is a hybrid scalable virtual model and has a skeleton that is formed as a multi-body structure (MBS); therefore, it can be easily positioned in various seating postures such as upright, reclined, lying down, etc. The skeleton is connected to deformable segments which represent the model's outer skin [9, 30, 31]. One can model a wide spectrum of occupants depending on their gender, height, weight and age by using the Virthuman.

2   Method

The Virthuman model and seats which represent the vehicle interior are generated in the Visual Environment (VE) and calculated in the Virtual Performance Simulation (VPS) environment, the PAM-Crash module. Virthuman in this study models a 6-year-old male with 124.75 cm height and weight of 23 kg (53rd percentile male) [16]. The body is located on a simplified child seat model. As far as the height of the child model is concerned, it is shorter than 145 cm, a child seat must be used for it [24] and is put on the vehicle seat. The child model is in an upright seating posture. The vehicle seat is also in an upright posture and its back angle with the global vertical axis (-z) in the VPS environment is 15.43 degrees.

For simulation simplicity reasons, the child seat is modelled by a shell frame made from ABS and has a 10 mm thickness. 40 mm polyurethane foam [26] covers the inner part of the frame. Its total weight is around 9.3 kg. The child seat was put on a vehicle seat which is also deformable [26]. The vehicle seat's geometry is based on the driver's seat of the Volvo XC70 Station Wagon [18] and its total weight is slightly more than 28 kg.

The foam is modelled using a general nonlinear strain-rate material in the VPS environment. It is a highly compressible non-linear elastic foam with strain-rate dependency and optional energy absorption (hysteresis). The foam behavior is described by two compressions and tension stress curves versus engineering strain, Figure 1. Its Young's modulus and unloading energy dissipation factors are 0.02 GPa and 0.25 respectively.
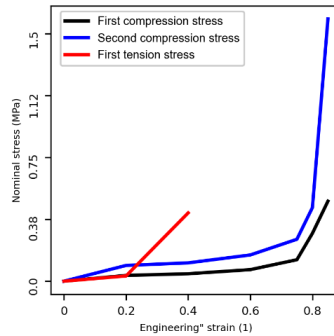
Figure 1
Polyurethane foam material

The child seat is connected to the vehicle seat with three elastic bars (a bar is on top of the child seat and two others are located on its back bottom) which have a 10 mm diameter. The inappropriate motion of the child seat, i.e., excessive bending of its back, is prevented by these bars.

Due to the usage of a deformable material in the present study for seats, a pre-simulation (free-fall) had to be done first to deform foam initially with the child's weight. Thus, the body model was released slightly above the seat from rest. The gravity acceleration is applied to all model nodes including the body, the child and the vehicle seats. By the end of pre-simulation nodes of the child model and seats are mapped to the initial model for representing the deformed models.

Instead of the seat's internal structure, the motion of chosen nodes under the seat cushion, back, headrest and armrest are fixed, Figure 2. Pure gravity acceleration was applied to the whole model along the z-axis for 500 ms as a pre-simulation, which was quite enough for the model to reach a stable position and deform the foam completely, as is shown in Figure 2.
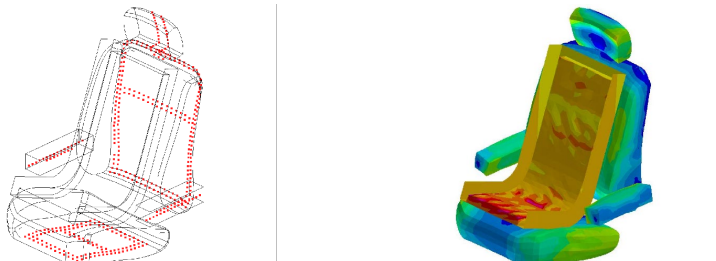

Figure 2
Vehicle seat. (Left) fixed nodes on the seat. (Right) deformed seat (pre-simulation).

Three child restraint systems (CRSs) that were selected for fastening the body to the seat are given in Figure 3.

Figure 3

Different restraint systems. (Left) three-point seatbelt. (Middle) four-point. seatbelt (Right) safety vest.

The first case is an integrated standard continuous three-point belt. It has three key components: connecting bars, and shoulder and lap membranes. This type of seatbelt is connected to a vehicle structure at three points: D-ring, Buckle and Anchor. The shoulder belt is started from the D-ring and passes over the trunk diagonally from upper left to lower right (from D-ring to Buckle). Meanwhile, the lap belt is located over the belly from right to left (from Buckle to Anchor). Non-linear bars are used to connect the free ends of membranes to external parts of a seatbelt (Retractor, D-ring, Buckle and Anchor). The nonlinear bar segment starts from the retractor, passes through the D-ring and ends at the upper part of the shoulder membrane. Another nonlinear bar part connects the shoulder and lap membranes via the Buckle. Finally, the bar segments connect the other side of the lap belt to the Anchor. Restraint systems that are considered for the present study are made from standard seatbelt materials, Figure 4. The membrane belt's width is 40 mm and its thickness is 1.2 mm.
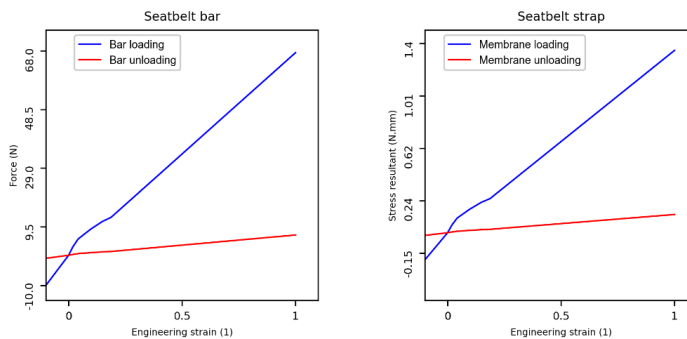

Figure 4

Seatbelt material. (Left) Seatbelt bar. (Right) Seatbelt strap.

A four-point seatbelt is the second restraint system which was considered in the present study for fastening the child model to the child seat. In the four-point seatbelt, membranes are attached to the child seat frame at four points by nonlinear bars rather than to the vehicle structure. The membrane material and bar material are the same as what is used for the three-point seatbelt. The safe tools in

the Virtual Performance Simulation (VPS) environment were used for generating three- and four-point seatbelts.

The third restraint system chosen is a conceptual design that is called a safety vest. The vest model has two panels which are attached to the child seat sides. The safety vest's panels are connected right in front of the model chest by a zipper. The safety vest is made from standard seatbelt material with 1.2 mm thickness the same as the three- and four-point seatbelts. The vest zipper is modelled by bars whose material properties are identical to the nonlinear bars used in the three-point seatbelt. The safety vest was fitted to the model skin's outer surface. The minimum initial vest offset is approximately 1mm between the thorax's side part and the safety vest panels, while the maximum initial offset is 9 mm and is between the thorax's frontal part and the safety vest's panels.

3   Crash Simulation

Since 2016, in accordance with the Euro NCAP regulations, larger child occupant dummies have to be considered for side crash tests [8]. The side crash test can be done by applying a crash pulse either to the model [21] or the impact barrier [27]. For evaluating passive safety system performance, i.e. seatbelts and airbags, it is common to use sled tests [10]. Either a full car body or a part of it, depending on the research goal, is located on a rail and the same deceleration pulse is applied to the model. Whenever occupants are situated in lightweight vehicles, side crash scenarios are a challenging issue, because they are faced with high-value pulses [27]. The Euro NCAP side-impact barrier crash acceleration pulse is used for simulating a side crash, Figure 5 [12, 23].
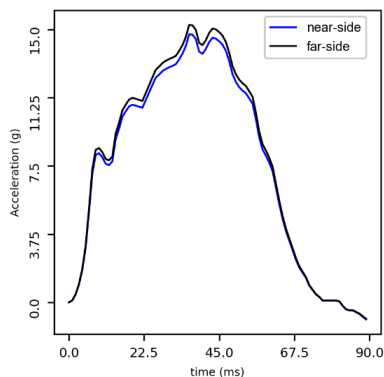

Figure 5

Acceleration pulse

For simulating a near-side crash, the acceleration pulse is applied horizontally to the model's center node along the global y-axis in the VPS. This center node is in connection with fixed nodes, Figure 2, as multiple nodes to one node constraint (MTOCO). The model's center node is just free to move along the y-axis (the crash axis); meanwhile, its other degrees of freedom are fixed. The three-point seatbelt parts are not symmetric like the two other restraint systems (four-point seatbelt and safety vest). Therefore, a far-side crash test must also be done. For this test, the acceleration pulse is applied horizontally to the model's center node along the global y-axis but in the negative direction.

4   Body Part Injury Assessment

A program is available for the Virthuman model to do post-processing and assess the particular model part (head, neck, thorax, abdomen, pelvis, femurs, knees and tibiae) injury level [15]. The injury level of each part is computed according to its kinematics and kinetics during the crash. Accelerations, forces and displacements are measured for joints that connect Virthuman's outer surface to its MBS structure. For instance, the head's center of gravity is selected to store the acceleration component and subsequently, the head injury criterion (HIC) is computed based on the absolute value of the head's acceleration. A model's neck injury level is determined by measuring three factors: flexion/extension moment, tension/compression and shear force of the neck joint. Deflections of segments on the model's thorax are measured during the simulation and compared with the existing injury criteria database for evaluating the thorax's injury level. The abdomen and pelvis injury levels are found based on compression and pubic forces respectively. Compression force and moment are collected for femurs and tibiae parts to determine these parts' injury levels. The injury level of knee parts is measured according to their joint's moment.

From the literature, injury criteria metrics are available for Virthuman's body parts (a 6-year-old child, a 20-year-old and a 100-year-old adult) [7, 11, 17]. It has already been mentioned that Virthuman is a scalable model. Therefore, the injury criteria are interpolated linearly according to the current passenger age at first by the post-processing program. Later on, either kinematic or kinetic data that were collected for body parts as output time-dependent variables are compared to the modified injury criteria for each body part. A body part injury level for a specific time is the worst injury level of a body part in the time interval from the beginning of the simulation to that time [14].

The overall injury level is graded at four basic levels (color-coded) in the software viewer in a similar way to the Euro NCAP consumer rating [6]. Either a small degree of injury or none is given by "Good". An injury level can also be "Acceptable" or "Marginal". However, injuries are shown by the "Poor", which

represents a very serious degree of injury, Figure 6. For instance, a head injury criterion is determined based on the HIC36 value. If it is lower than 650, a "Good" level is assigned to the head and it is represented by a "Green" color on the model in the VPS visual environment (VE). In contrast, in a case where HIC36 is more than 1000, the program returns "Poor" and colors the head in VE with "Red". All body injury criteria are available in [15].
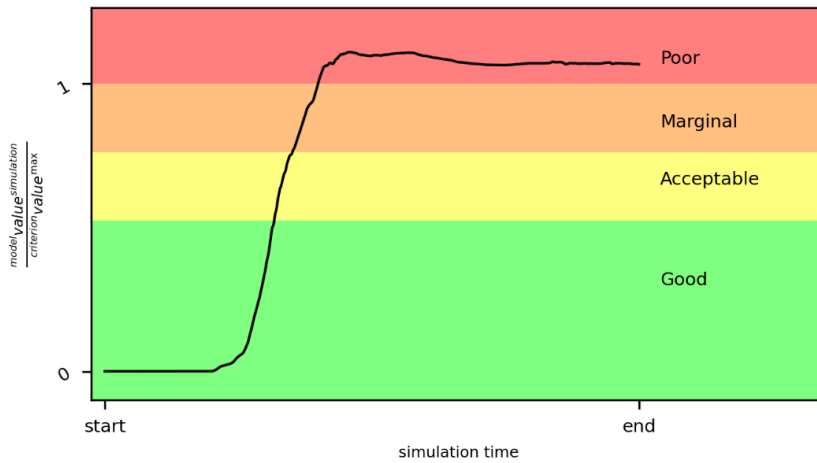

Figure 6
Injury assessment for a body part

5   Discussion

The kinematics of the child occupant body for the side crash tests (near- and far-side) are illustrated in Figure 7, regarding the three restraint systems.
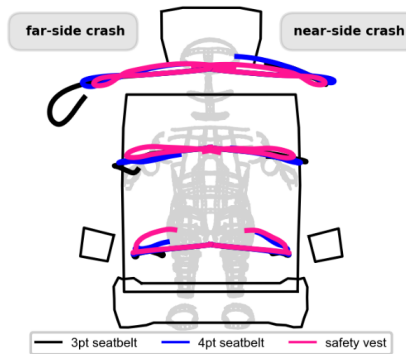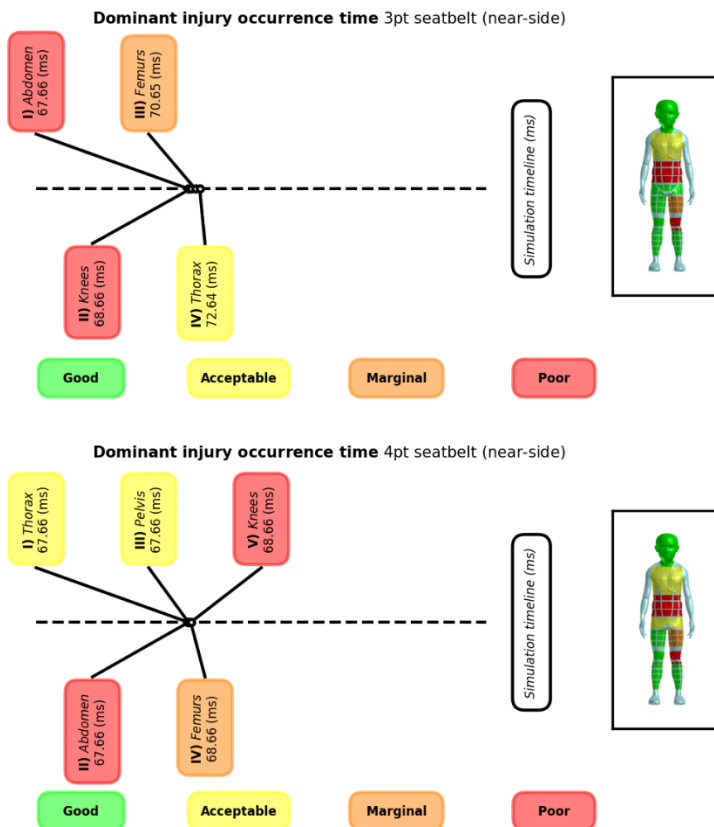

Figure 7
Child occupant kinematics in side collisions with different restraint systems

Curves in plots show the trajectory of nodes on the head center, sternum and hip in crashes. The curves which are located on the right side of the figure illustrate the trajectory of mentioned nodes in the near-side crash. The nodal trajectory on the left side of Figure 7 relates to these nodes in the far-side crash. For restraint systems that have symmetric geometry (four-point seatbelt and safety vest) Figure 3. The body's kinematic response is also symmetric in near- and far-side crashes Figure 7. The three-point seatbelt does not have symmetric geometry; hence, the body's kinematic responses are not symmetric in side crash scenarios Figure 7. Therefore, from now on body injuries are discussed for restraint systems in the near-side crash and far-side crashes with a three-point seatbelt.

The occurrence time of the final injury level – the dominant one – per body part is illustrated in Figure 8 for each restraint system. The simulation timeline is represented with a horizontal dashed line. Body parts with a "Good" injury level are not shown in occurrence time plots and the plot just shows injury occurrence times for the parts which have other level injuries, i.e., "Acceptable", "Marginal" and "Poor".

Dominant injury occurrence time 3pt seatbelt (near-side)

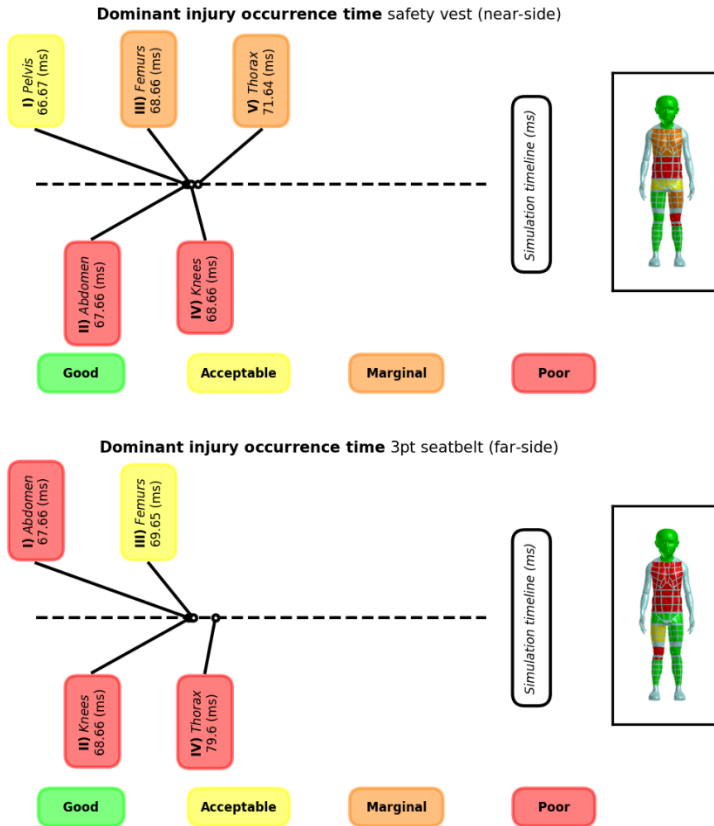**Dominant injury occurrence time** 4pt seatbelt (near-side)

Figure 8

Dominant injury criteria occurrence time for a model in the side crashes

A detailed vehicle interior is not considered in this study and the body is subjected to side crash pulses; hence, the model head moves laterally and does not collide anywhere. In consequence, there is no sudden jump in the head acceleration curve versus time. Therefore, the head injury criterion (HIC36) is 44.89, 45.34 and 59.1 for the three-point seatbelt, four-point seatbelt and safety vest in the near-side crash, respectively. HIC36 is 52.7 for the model with a three-point seatbelt in the far-side crash Figure 9. All of these values are lower than 650 [15]; hence, the head injury level for these test occasions is "Good" and is indicated by "green" in the software viewer Figure 8.
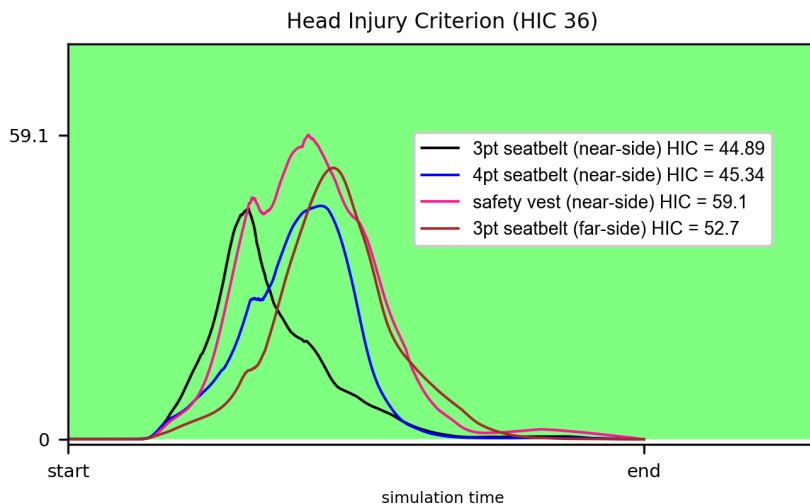
Figure 9
Non-dimensional neck extension moment in relation to simulation time

Information can be found in the colored boxes pointing to the timeline with a dark line. The injury sequence for a part is given in roman numerals. The first moment a part's dominant injury started is also given in the boxes. As an example, in Figure 8, with the three-point seatbelt in the near-side crash, the abdomen and knees reach "Poor" injury levels at 67.66 and 68.66 ms, respectively. Its femur injury level will be "Marginal" since it is 70.65 ms while the thorax reaches an "Acceptable" injury level of 72.64 ms. For ease of viewing, rounded numbers are put in the boxes. From the dominant injury occurrence time point of view, the majority of the body parts face a level of injury at around 70 ms with a side crash. The simulation's time, as well as the duration of the crash pulse's time, is 200 ms. Comparing dominant injuries in near-side crashes indicates that the most severe of injuries involve the knees and abdomen, with "Poor" levels and occur around 68 ms.

For side crashes, the model is subjected to lateral motion and bends to its side as a consequence of the inertia distribution. Restraint systems restrict the abdominal and thoracic motions but the difference between the model's trunk and head inertia generates a moment on the model's neck. The neck moment in the sagittal plane concerning simulation time is illustrated in Figure 10. None of the moment curve related to restraint systems exceeds the "green" band and the post-processing algorithm detects the "Good" injury level for the neck that can be seen in Figure 10.
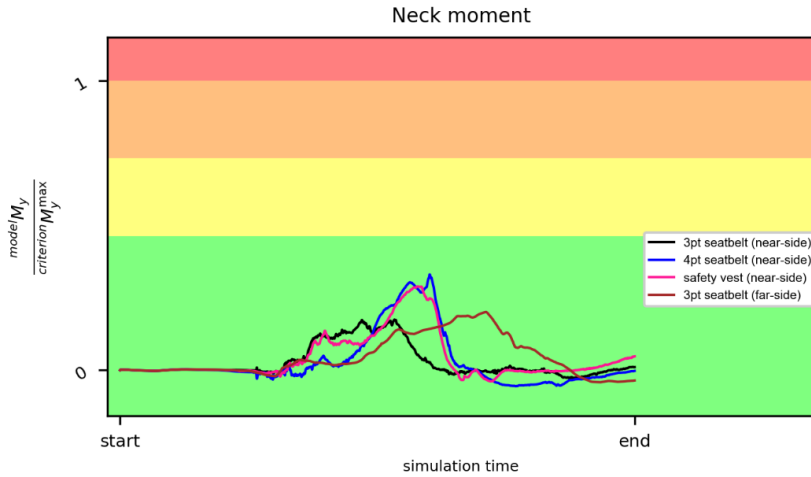
Neck moment

Figure 10

Non-dimensional neck extension moment in relation to simulation time

The post-processing takes the thorax deflections at frontal and side segments into account to determine the injury level of the thorax. Variations of the thorax deflection vis-a-vis simulation time are given in Figure 11. There are several segments on the Virthuman thorax. A thorax segment, which has the highest deflection peak is illustrated in Figure 11, as it is the most effective part for determining the thorax injury level. From the plots, it is seen that a model that has a three-point seatbelt, has the worst injury level, "Poor", in the far-side crash Figure 8.
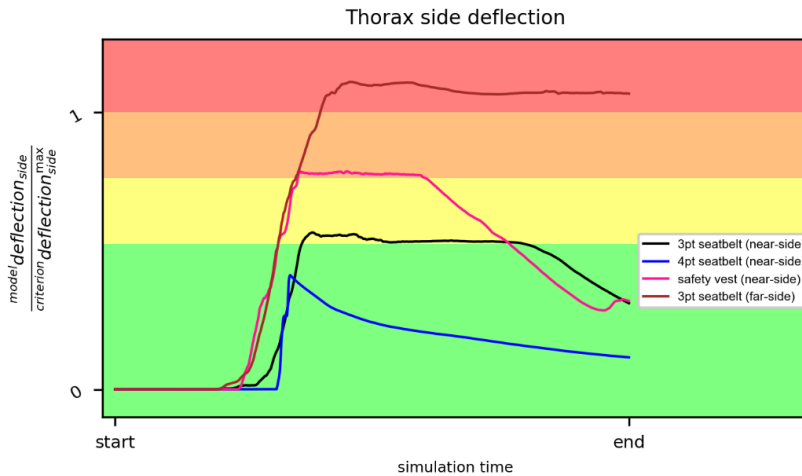
Thorax front deflection
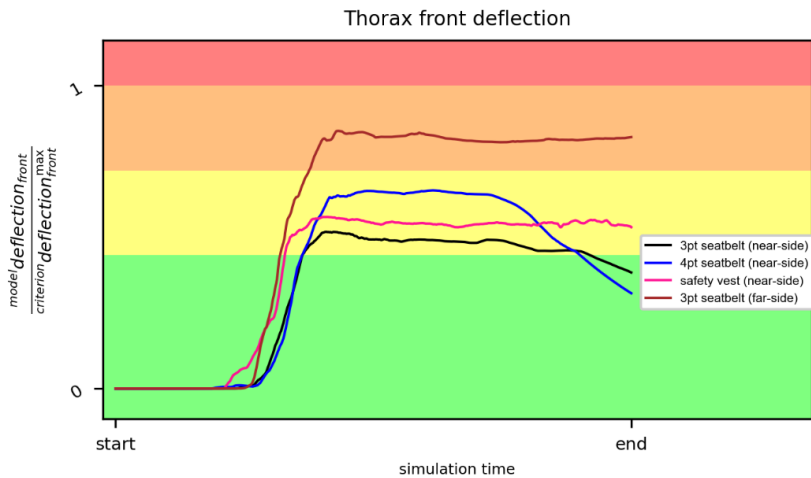
Figure 11

Non-dimensional thorax deflection in relation to simulation time. (Up) frontal segments. (Down) side segments.

This is the result of a large deflection on the thorax side segment Figure 11. The model with a safety vest in the near-side crash has a "Marginal" injury level because of the thorax deflection that is in the "brown" band. For the rest of the test cases, the "Acceptable" injury level is assigned to the thorax because a part of the thorax response curve is located in the "yellow" band.

Variation of the compression force for an abdominal segment in relation to simulation time is plotted in Figure 12. This segment has the highest compression force peak value among the other abdominal segments. Hence, its effect in determining the abdomen's injury is more than with other segments. Comparing the abdominal non-dimensional force regarding different restraint systems indicates that none of these restraint systems can provide a safe condition for the model from an abdominal injury point of view. Hence, in Figure 8 the abdomen is shown in "red".
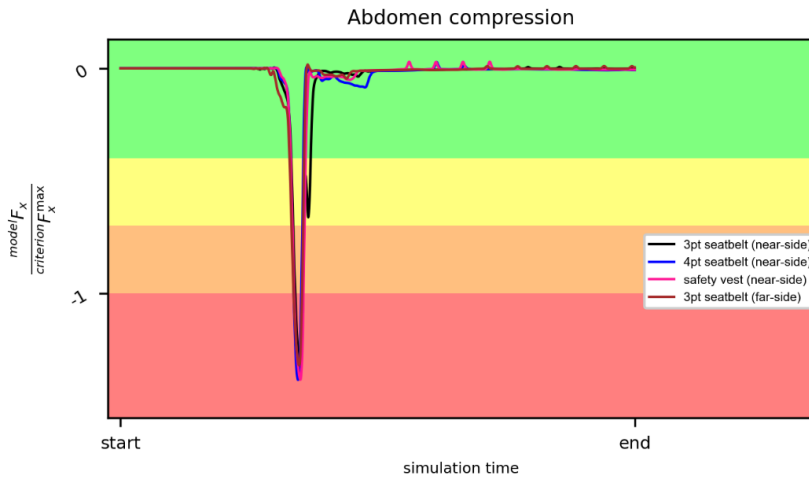
Figure 12
Non-dimensional abdomen compression in relation to simulation time

The pubic force in relation to simulation time is demonstrated in Figure 13 for each restraint system. The three-point seatbelt in the far-side crash has the best reaction compared to the others. When the near-side crash is the test's concern, the three-point seatbelt reaction is acceptable and keeps the pubic force peak in the "Good" injury level domain. However, the pubic force peak for the four-point seatbelt and safety vest is slightly located in the "yellow" band and the post-processing program indicates an "Acceptable" injury level for the model pelvis in these scenarios.

In Figure 14, one has the variation of the femoral moment in relation to simulation time. All of the restraint systems act quite similarly in the near-side crash and the femur injury level is determined as "Marginal" by the post-processing algorithm. The three-point seatbelt shows a better reaction in far-side crashes, as the femoral injury level is "Acceptable", which is better than the others in a near-side crash.

The knee joint moment variation in relation to time is illustrated in Figure 15 for different restraint systems. It is seen that the curves' peaks are in the "Red" zone and the knees' injury level for all restraint systems is "Poor". The type of restraint system has no considerable effect on knee injuries because it cannot restrict the motion of the body's lower extremities.

The post-processing algorithm deals with tibiae moment in relation to simulation time to evaluate their injury level. According to Figure 16, when either model is subjected to a near- or far-side crash, its tibiae injury level will be "Good" and restraint system types act in a similar way.
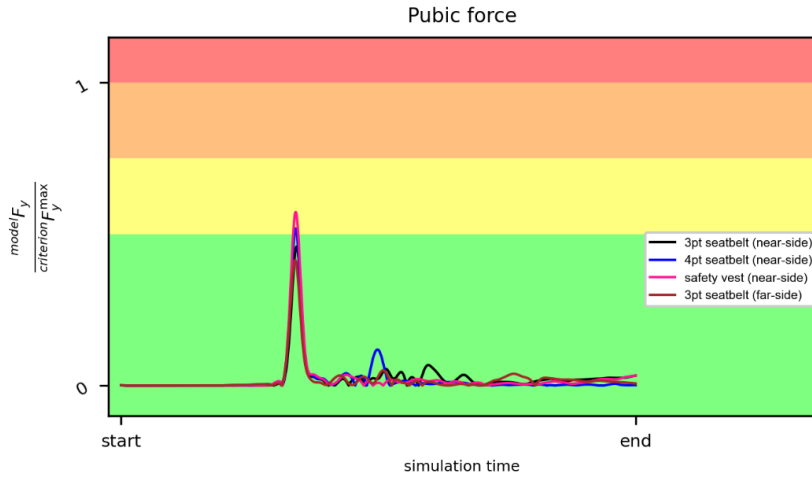
Pubic force

Figure 13

Non-dimensional pubic force in relation to simulation time
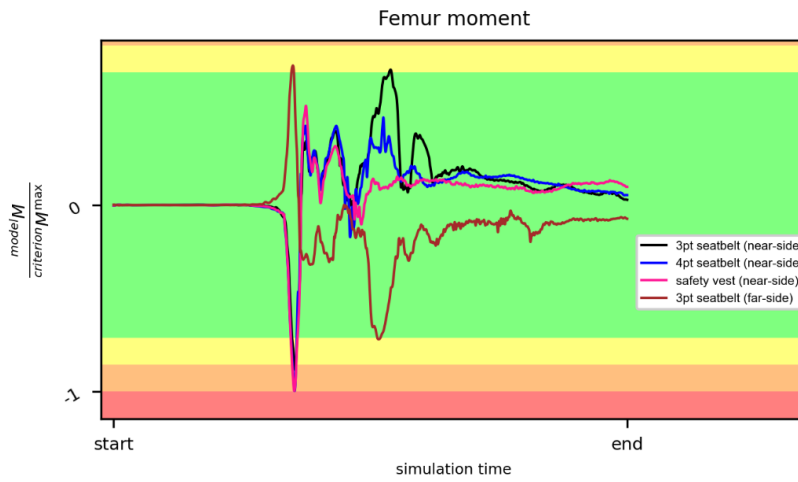
Femur moment

Figure 14

Non-dimensional femoral moment in relation to simulation time
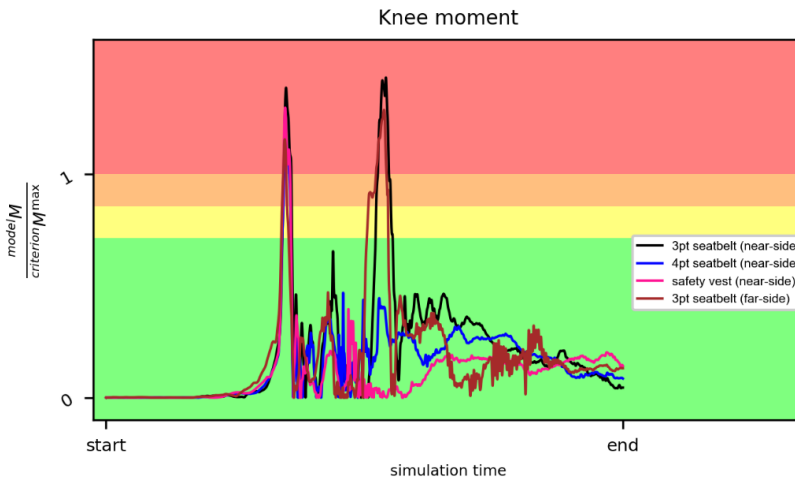
Knee moment

Figure 15

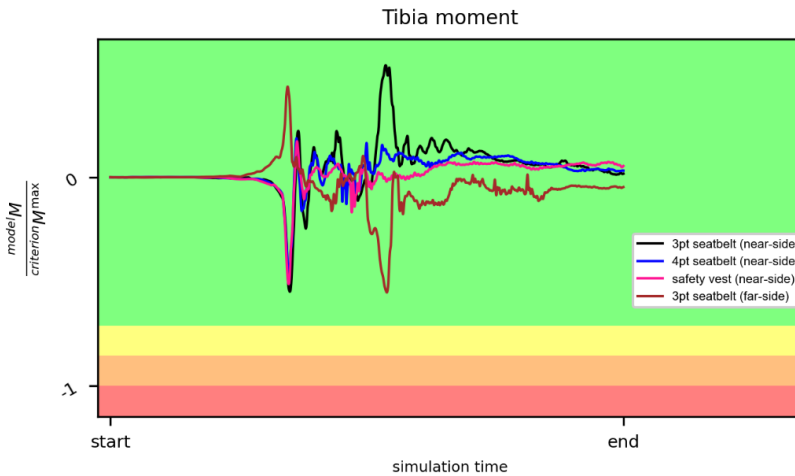Non-dimensional knee moment in relation to simulation time

Tibia moment

Figure 16

Non-dimensional tibia moment in relation to simulation time

The safety restraint systems in the present study are made from standard seatbelt materials, Figure 4, and their thickness is 1.2 mm. The sectional force of a belt or safety vest is measured for a section on the top left of the strap. Figure 17 shows the position of the section in red for the three-point seatbelt as an example of where strap force is recorded during the crash simulation. The variation of section forces in relation to the time is given in Figure 18 for different restraint systems. Because the force is distributed over a wider area (the contact area between the restraint system and the child's thorax) it causes lower force applies to the four-

point seatbelt and safety vest strap, that attaches the vest to the seat structure, in comparison with the three-point seatbelt. It can be seen that the section forces' peak for three- and four-point seatbelts are almost three times higher than is measured for a safety vest.
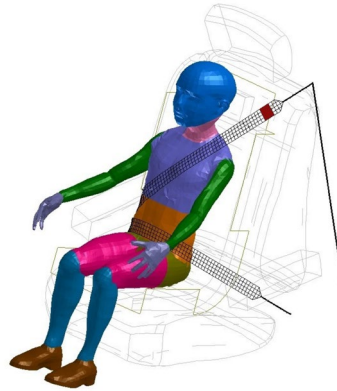

Figure 17

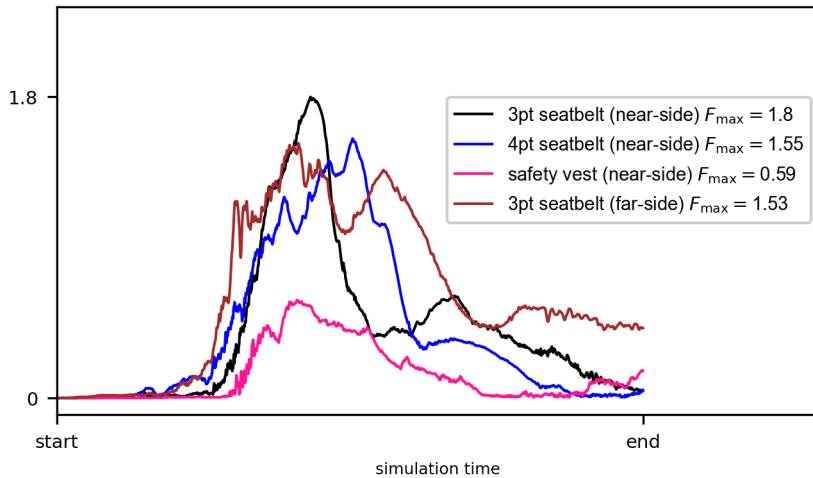Strap section force position

Figure 18

Strap section force

Seatbelts (three- or four-point seatbelts) and safety vest are not the only components which restrict a child's model motion. The child model is on a seat made from polyurethane foam that absorbs a part of crash energy. When the child model has either a four-point seatbelt or safety vest, the motion of the child's thorax is restricted more effectively than on occasion it has a three-point seatbelt.

The amount of crash energy that is dissipated by the seat's foam in these cases is relatively lower than the test case done by a three-point seatbelt. It happens because a child is fastened by the four-point seatbelt and safety vest its trunk has less lateral rotation than a case it has a three-point seatbelt.
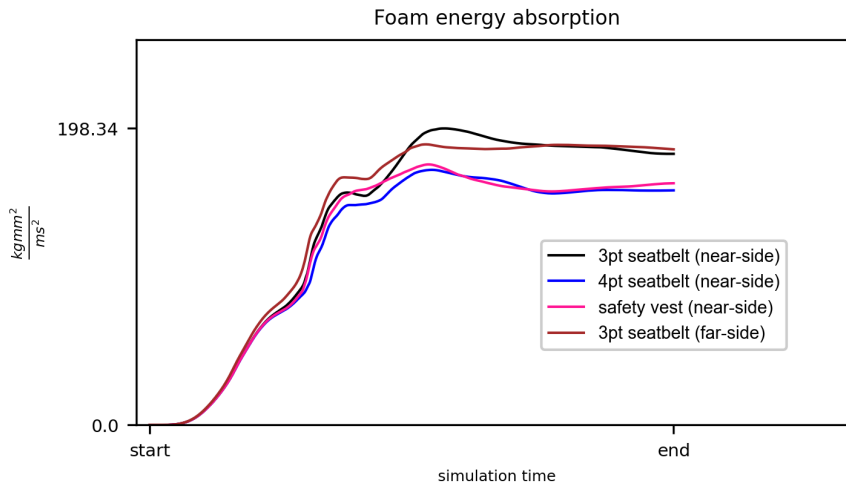

Figure 19
Seat energy absorption

Conclusions

A comparative study was completed to consider the influence of using three restraint systems, for a child occupant, in a side crash. A 6-year-old (53rd percentile male) reference Virthuman model is scaled to represent the child as a model. The body was in a simplified child seat, that is positioned above a deformable vehicle seat. Seats are made from polyurethane foam. The simulation was run in the Virtual Performance Simulation (VPS) environment first and an algorithm which is available for Virthuman processed the results to determine the injury level for particular body parts. The symmetrical geometry of the four-point seatbelt and safety vest causes the kinematics of the body in near- and far-side crashes to be symmetric as well. But the three-point seatbelt's geometry is not symmetric like the other restraint systems. Therefore, it is expected not to have symmetric kinematic curves, for a body in near- and far-side crashes. From the particular injury level point of view, a four-point seatbelt and safety vest cannot provide safer conditions for a child model encountering a side crash, in comparison with a model, which has a three-point seatbelt. However, by using a four-point seatbelt, a delay occurs in the thorax injury, which helps other safety means to reduce injuries to the body. The safety vest geometry is shown, in this study, not to have an appropriate design. Therefore, it allows serious pelvis injury to occur and is not as good as the three-point seatbelt.

References

[1] *Car Seat Recommendations for Children*. Available from: https://www.nhtsa.gov/equipment/car-seats-and-booster-seats.

[2] Arbogast, K. B., et al., *Child occupant protection: a summary of current safety recommendations.* Primary care update for Ob/Gyns, 2001. **8**(4): p. 141-148.

[3] Baker, G., et al. *Kinematics and shoulder belt engagement of children on belt-positioning boosters during emergency braking events.* in *The International Conference on the Biomechanics of Impact (IRCOBI)*. 2017.

[4] Ebel, B. E. and D. C. Grossman, *Crash proof kids? An overview of current motor vehicle child occupant safety strategies.* Current problems in pediatric adolescent health care, 2003. **33**(2): p. 38-55.

[5] Elliott, M. R., et al., *Effectiveness of child safety seats vs seat belts in reducing risk for death in children in passenger vehicle crashes.* Archives of pediatrics adolescent medicine, 2006. **160**(6): p. 617-621.

[6] EuroNCAP, ASSESSMENT PROTOCOL – ADULT OCCUPANT PROTECTION, 9.1.2, 2020.

[7] Forman, J. L., et al. *Fracture tolerance related to skeletal development and aging throughout life: 3-point bending of human femurs.* in *The International Conference on the Biomechanics of Impact (IRCOBI)*. 2012.

[8] Holtz, J., et al. *Side-impact simulation study to investigate the protection of older child occupants in lightweight vehicles.* in *The International Conference on the Biomechanics of Impact (IRCOBI)*. 2016.

[9] Hyncik, L., et al., On scaling virtual human models, 2013.

[10] Jimenez, M., et al., *Finite element simulation of mechanical bump shock absorber for sled tests.* International Journal of Automotive Technology, 2015. **16**(1): p. 167-172.

[11] Kleinberger, M., et al., *Development of improved injury criteria for the assessment of advanced automotive restraint systems.* 1998. **4405**(9): p. 12-17.

[12] Léost, Y. and M. Boljen. *Crash simulations of electric cars in the EVERSAFE project.* in *COMPLAS XIII: proceedings of the XIII International Conference on Computational Plasticity: fundamentals and applications*. 2015. CIMNE.

[13]   Luttenberger, P., et al., *Assessment of future occupant restraint principles in autonomous vehicles.* The International Conference on the Biomechanics of Impact (IRCOBI), 2020.

[14]   Mecas, Virthuman Postprocessing Manual (VPS Explicit MBS Model, Model Version 1.1) Rev. 1, 2016.

[15]   Mecas, Virthuman Postprocessing Manual (VPS Explicit MBS Model, Model Version 1.5) Rev. 1, 2020.

[16]   Mecas, Virthuman User's Manual (VPS Explicit MBS Model, Model Version 1.5) Rev. 1, 2020.

[17]   Mertz, H. J. and L. M. Patrick, *Strength and response of the human neck.* 1971: p. 2903-2928.

[18]   Ozmumcu, S. *Volvo xc7 Station Wagon Seat*. 2012   [cited 7-8-2012]; Available from: https://grabcad.com/library/automobile-seats.

[19]   Paiman, N. F., et al., *A study on the use and misuse of child restraint system (CRS) in Malaysia.* Journal of the Society of Automotive Engineers Malaysia, 2018. **2**(1): p. 5-13.

[20]   Peden, M. P., et al., *World report on child injury prevention*. 2008, Geneva, Switzerland.

[21]   Pintar, F. A., et al. *Worldsid assessment of far side impact countermeasures*. in *Annual Proceedings/Association for the Advancement of Automotive Medicine*. 2006. Association for the Advancement of Automotive Medicine.

[22]   Posuniak, P., et al. *Child restraint systems: problems related to the safety of children transported in booster seats (without integral safety belts)*. in *2018 XI International Science-Technical Conference Automotive Safety*. 2018. IEEE.

[23]   PROGRAMME, E.N.C.A., FAR SIDE OCCUPANT TEST & ASSESSMENT PROCEDURE, 2022.

[24]   Reed, M. P., et al., *Effects of vehicle seat and belt geometry on belt fit for children with and without belt positioning booster seats.* Accident Analysis and Prevention, 2013. **50**: p. 512-522.

[25]   Schroeder, P. A., *The Effects of Child Restraint System Use and Motor Vehicle Collision Severity on Injury Patterns and Severity in Children 8 Years Old and Younger*. 2018.

[26]   Špirk, S., M. Křížek, and Š. Jeníček. *Polyurethane foam behaviour during impact*. in *MATEC Web of Conferences*. 2018. EDP Sciences.

[27]   Stein, M., et al. *Concept for lateral Impact Protection of a centred Driver in a light Electrical Vehicle*. in *The International Conference on the Biomechanics of Impact (IRCOBI)*. 2014.

[28]   Tarriere, C. *Children are not miniature adults*. in *Proc. of Int. Conf. on the Biomechanics of Impacts (IRCOBI)*. 1995.

[29]   Transportation, U.S.D.o., National Highway Traffic Safety Administration (NHTSA) (2001) Traffic Safety Facts 2001. Children (DOT HS 809 471)

[30]   Vychytil, J., et al., Prediction of injury risk in pedestrian accidents using virtual human model VIRTHUMAN: real case and parametric study, 2016.

[31]   Vychytil, J., et al., Scalable multi-purpose virtual human model for future safety assessment, 2014.